practical application. In the present work, we use 260 keV H^+ ion irradiation to a fluence of 5.0×10^{15} cm^{-2} at room temperature. Though almost no effects of H irradiation on an amorphous layer are formed in He-implanted 6H-SiC, the significant recrystallization of He-implanted 4H-SiC with a relative damage of 0.55 occurs after H irradiation. This is very useful for practical applications. For example, in the nuclear radiation environments, dense energetic H and He atoms are produced simultaneously. Therefore, the He implantation-induced defects can be annealed out upon H irradiation immediately, indicating that the amorphous phase has never been formed under such a condition. The present experimental results demonstrate a strong reduction of the damage production to extend SiC material lifetime in nuclear reactors.

References

[1] V. Heera, J. Stoemenso, R. Koler, et al., J. Appl. Phys., 77(1995)2999.
[2] Y. W. Zhang, R. Sachan, O. H. Pakarinen, et al., Nat. Commun., 6(2015)8049.

4 - 3 An Experimental Setup for High Temperature and High Pressure Fluid Flow Effects

Ma Zhiwei, Wang Zhiguang, Liu Chao, Sun Jianrong, Chang Hailong, Li Bingsheng, Sheng Yanbin and Pang Lilong

In order to accumulate the experimental data for building accelerator driven sub-critical systems (ADS), a high temperature and high pressure water circuit setup has been built. It is mainly used to study heat transfer deterioration of high temperature and high pressure water vapor in the circuit, flow instability mechanism and heat exchange efficiency of fuel rod in primary loop. Lots of similar experimental setups have been built by scientific research institution around the world[1−3]. Unlike the existing experimental setup, flow rate of high temperature and high pressure water vapor was considered as a significant parameter to study above-mentioned research proposal.

The operating temperature of the experimental setup was designed to be 300 ℃∼650 ℃ and the operating pressure is 8∼10 MPa. The main parameters of the experimental setup are shown in Table 1.

Table 1 The relevant parameters of the experimental setup.

Parameters	Values
Operating temperature/ ℃	300∼650
Operating pressure/ MPa	0.1∼10
Flow rate/(m/s)	0∼10
The conductivity of deionized water/ (µs/cm)	≤ 0.1
The dissolved oxygen content of deionized water/ppb	≤ 10
Inlet temperature/ ℃	300
Length of test section/mm	1 500

The flow chart of setup shown in Fig. 1 and the side view of setup shown in Fig. 2.

The experimental setup consists of three components:

1) Deionized water preparation and deoxidization system: Deionized water was prepared by deionized water preparation machine and the conductivity of water can be less than 0.1 µs/cm. Then deionized water was deoxygenized by injecting nitrogen to make the oxygen content below 10 ppb and the dissolved oxygen content can be controlled by nitrogen feedback regulation.

2) Heating and experimental system: Deionized water was pumped into circulation loop by a high-pressure plunger pump. The water was preheated up to 300 ℃ by electro-magnetic induction furnace and then heated by heating pipe in chamber. Thermometer probes and piezometers were set in the loop to collect data.

3) Experimental control and data collection system: The experimental setup was controlled by a control cabinet and software on computer. Experimental data can be real-time acquired by software.

Some tests have been done when flow rate was set as 5 m/s and 8 m/s. It turned out that the experimental setup can run stably. The mid-section steam temperature can reach up to 360 ℃ and remained stably when flow rate was 5 m/s (Fig. 3(a)). The medium-frequency heating power was 7.5 kW at the beginning and then decreased to 2.0 kW after heating for 70 min (Fig. 3(b)). The mid-section steam temperature can reach up to 350 ℃ when flow rate was 8 m/s(Fig. 4(a)). The medium-frequency heating power was 22 kW and maintain steady basically (Fig. 4(b)).

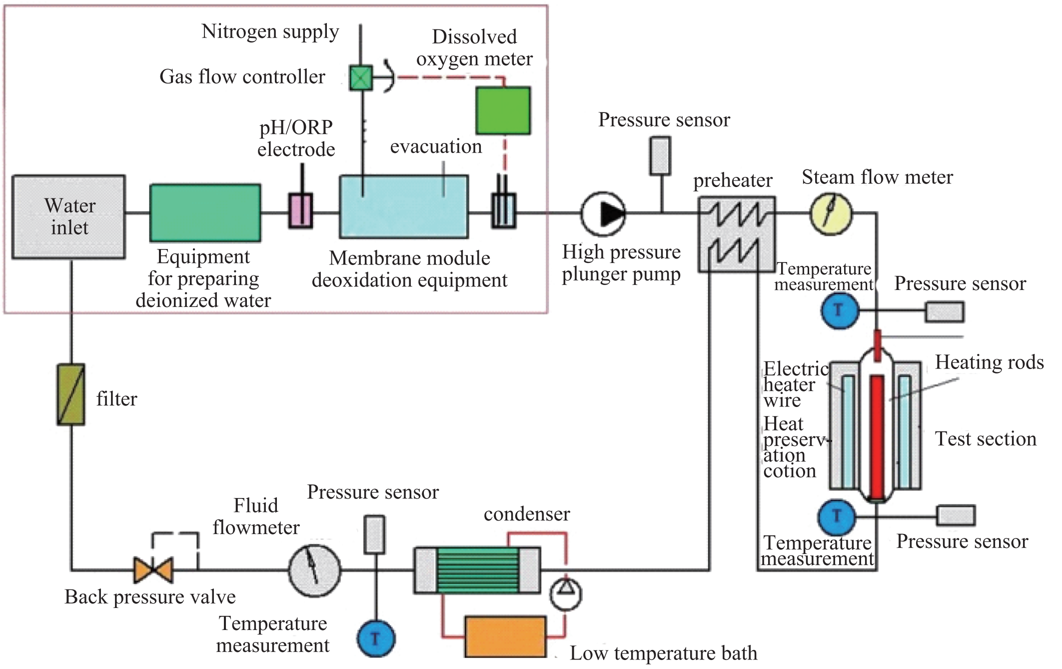

Fig. 1 (color online) Flow chart of the experimental setup for high temperature and high pressure fluid flow effects.

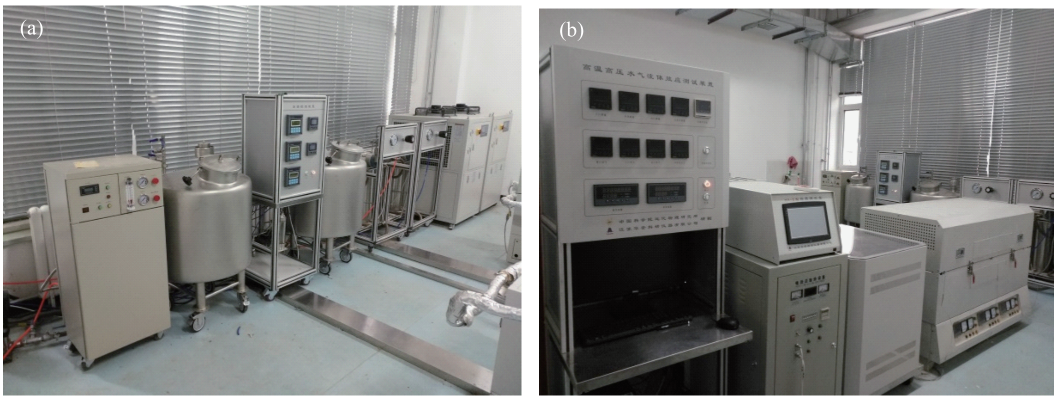

Fig. 2 (color online) Side view of setup: (a) deionized water preparation and deoxidization system; (b) heating and experimental system& experimental control and data collection system.

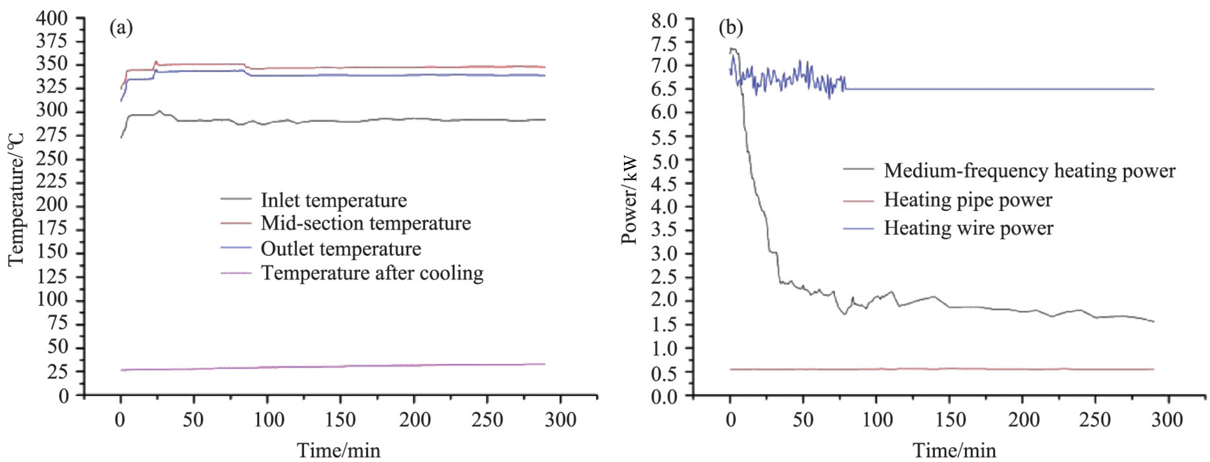

Fig. 3 (color online) Steam temperature(a) and heating power(b) change over time when the flow rate was 5 m/s.

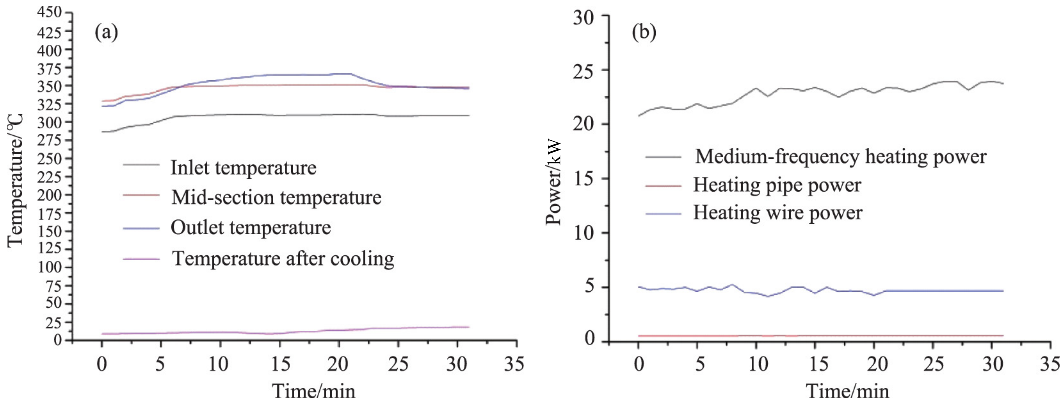

Fig. 4 (color online) Steam temperature(a) and heating power(b) change over time when the flow rate was 8 m/s.

References

[1] M. Suzuki, H. Nakamura, A study on ROSA/LSTF SB-CL-09 test simulating PWR 10% cold leg break LOCA, JAEA-Research[R]. Japan: Atomic Energy Agency, (2008).

[2] N. Jose, J. Reye, Nuclear Science and Engineering, 186(1998)53.

[3] D. L. Reeder, Loft system and test description, NUREG/CR-0247, TREE-1322[R]. [S.l.]: [s.n.], (1979).

4 - 4 Vacancy Like Defects in WFeNi Alloys Induced with H Ion Irradiation at 600 ℃

Cui Minghuan, Wang Zhiguang, Shen Tielong, Zhu Yabin, Pang Lilong, Li Bingsheng, Yao Cunfeng, Wang Dong and Han Yi

WFeNi alloys are extensively used in making penetrators against armor plates, balance supporting systems for airplanes and high-speed trains, blocking devices for radioactive- and X-rays, and containers for radioactive materials, *etc.*, due to its advantages such as high density, high strength, good machinability and ductility. The microstructure of WFeNi alloys after the irradiation of ions would change, which may affect the mechanical properties of the material. It is very meaningful to investigate this issue.

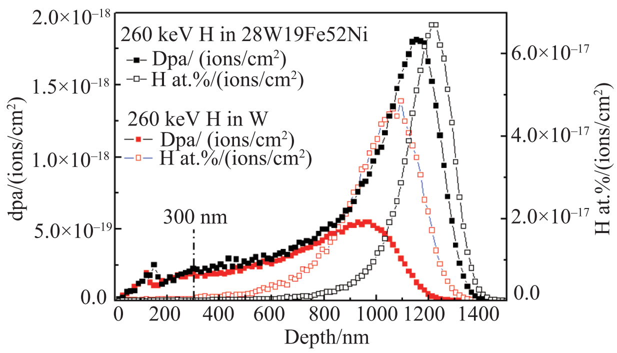

Fig. 1 (color online) The cross section profiles of dpa and H atom distributions in the two areas (*i.e.* pure tungsten area and 28W19Fe52Ni alloy area).

The samples used in the study were 93W4.5Fe2.5Ni (wt.%) alloys, which were consisted of two-phase microstructure of spherically-shaped tungsten particles with bcc structure distributed homogeneously in the W-Ni-Fe matrix (about 28W19Fe52Ni in wt.%) with fcc structure. The samples were irradiated with 260 keV H ions at 600 ℃. The irradiation fluences were 5.0×10^{15}, 1.0×10^{16}, 5.0×10^{16}, 1.0×10^{17} and 3.0×10^{17} ions/cm^2. The cross sections of dpa (displacement per atom) and H atom distributions in the two areas (*i.e.* pure tungsten area and 28W19Fe52Ni alloy area) of the samples were calculated with SRIM and shown in Fig. 1. It can be seen that the dpa cross sections and the H atom concentration cross sections in the two areas are almost the same in the first 800 nm and 500 nm from surface, respectively. The peak dpa cross section of the alloy is about 1.8×10^{-18} dpa/(ions/cm^2), which is higher than the value of pure tungsten (5.4×10^{-19} dpa/(ions/cm^2). The peak H concentration cross section of the alloys is about 6.7×10^{-17} %/(ions/cm^2), which is higher than the value of pure tungsten (4.6×10^{-17} %/(ions/cm^2)).

After H irradiation, the slow positron annihilation spectroscopy (SPAS) and coincident doppler broadening (CDB) spectroscopy are completed to investigate the vacancy like defects of the unirradiated and irradiated samples. The detected S and W parameters are fitted with the vepfit program. Fig. 2 (a) gives the detected S parameters as scattered points versus incident positron energies and the corresponding depths, and also the vepfit results as